Properties of Heterogeneous Material Using Fractional Models: Rubber Agglomerate Panel

Bruno Manuel Ribeiro Alves*

Independent Researcher, 6010 Charleroi, Belgium

* Correspondence: Bruno Manuel Ribeiro Alves (b.bruno.a@gmail.com)

Citation: B. M. R. Alves, "Properties of heterogeneous material using fractional models: Rubber agglomerate panel," *Power Eng. Eng. Thermophys.*, vol. 2, no. 2, pp. 86–96, 2023. https://doi.org/10.56578/peet020203.

Abstract: This paper aimed to analyze the properties of rubber agglomerate panel, a heterogeneous material. After making three adjustments using three classical differential fractional models, namely, the Scott-Blair model, the generalized fractional Maxwell model (FMM), and the 1D standard fractional viscoelastic order for fluids (SFVOF), this paper assessed the number of parameters in those models for rubber agglomerate panel, made from rubber grains and urea thermoplastic elastomer (TPE). Combining data published from an undergraduate thesis with Microsoft Excel software and the solver command, this paper obtained better sample results using four parameters, rather than two or three complicated material function equations. Data of Ribeiro Alves in 2019 came from hardness experiments. Then this paper transformed deformation data into creep compliance in accordance with equation $J(t) = \varepsilon/t$ (mm/s), and obtained graphical adjustment representations, parameter values, and eventually adjustment equations. However, results from the modified FMM and 1D SFVOF were more comparable, and certain hypotheses were investigated to choose the better model. It was determined that the generalized FMM fit the data the best for this time period. With a certain margin of error, this model could be used for constructing new recycled materials and rubber agglomerate panel using Salvadori equipment. However, it is suggested that new and recent materials should be tested in order to solve environmental problems.

Keywords: Rubber agglomerate panel; Scott-Blair model; Generalized fractional Maxwell model (FMM); 1D standard fractional viscoelastic order for fluids (SFVOF); Adjustment; Microsoft 365; Urea thermoplastic elastomer (TPE)

1 Introduction

Rubber agglomerate panel is made from rubber granules, water, and Methylenediphenyl Diisocyanate (MDI) through chemical reaction of polycondensation, because water reacts with an isocyanate group to generate a carbamic acid (Figure 1), which subsequently releases a small molecule of carbon dioxide and forms a functional group of primary amines in situ of isocyanate lateral group (Figure 2). The isocyanate lateral group then combines with this primary amine to create a urea functional group (Figure 3). Ongoing interactions between urea functional groups create biuret crosslinking (Figure 4) [1].

Rubber agglomerate panel is created using specialized equipment, such as Salvadori equipment from the Italian business, including a mixer, a press, and a silo to store the components [2]. Later quality control systems simulate the hardness property in accordance with precise models and data gathered. The material is in a state of compliance if the data matches the model.

Innumerous software tools are available now for modeling, such as Julia's RHEOS Package [3–5], R-statistics [6], Excel from Microsoft Office [7], Mathematica for fractional viscoelasticity [8], gnu Octave [9], MATLAB [10], Minitab [11], and SPSS [12]. However, this paper is not interested in studying the functions. Additionally, due to their specialized nature, it is sometimes crucial to learning to program using them in order to write material functions, based on static and dynamic experiments of differential fractional models.

In the initial stage of research, the author of this paper was engaged in a research and software development project, and modeled in-house ethylene-olefin resins using 1D standard Field of View (FOV) fluid [8]. The author published his first article, which discussed how to modify the property of metallocene-catalyzed polyethylene using statistical studies and dynamic models. Study of Doerpinghaus Jr [13] showed that this polyethylene was a homogeneous

substance devoid of additions. Later, Alves [6, 7] was eager to study software that was more suitable for his needs. After concluding his first assignment using Excel (Microsoft software), the author became more interested in open-source software and started using R Statistic, which is a powerful open-source statistical research program.
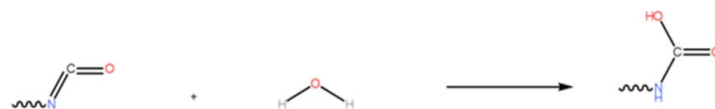
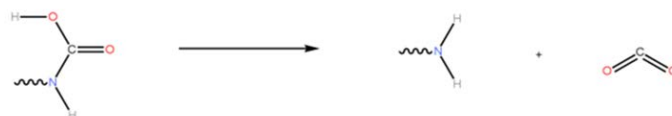**Figure 1.** Isocyanate group reacts with water to form a carbamic acid

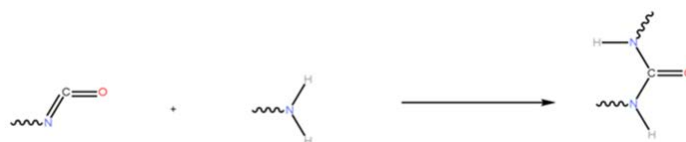**Figure 2.** Decarboxylation of carbamic acid forms a primary amine

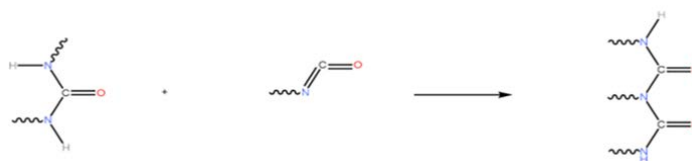**Figure 3.** Reaction forms urea functional groups

Figure 4. Reaction of urea functional groups forms biuret crosslinking

This paper chose mathematical tool with a specific model, because the tool ensured that physical property was described in the proper condition, which best met the author's goals. Innumerous models include the Newtonian and the Hookean models (represented by a dashpot and a spring) [14]. Considering viscosity and deformation, non-Newtonian inelastic models can be used to analyze the property of fluids. Other models include the power-Law model, the Bird-Carreau model, and even the Bingham fluids. These models are more complex and accurately depict the property of yaourts and gelee of fruits [15, 16].

Other models include traditional differential models and non-linear differential models, such as the PTT model, the Pom-Pom model, and the single eXtended Pom-Pom model [17]. Recent models include differential fractional models, integral fractional models, and integral models, such as the integral Maxwell model, which integrates the property as a time function, the Scott-Blair model, the generalized FMM, the Voigt model, the fractional Kelvin-Voigt model, the Zener fractional model, the Anti-Zener fractional model and the Burguers fractional model [18], which have derived other models and were referred later in this study.

Complex equations have been used to understand the property of experimental materials. Adjusted models should approximate theoretical results. Obviously, extremely complex equation should be used if the property is extremely complex.

Material property should be accurately predicted by the model, which is not always possible due to elastic retraction, die-swelling and first and second order normal stress differences (N1 and N2). The challenge of these models is how to interpret the findings.

Jaishankar and McKinley [19] developed the first differential model, which combined the Hooke and Newtons Law to represent a spring and dashpot discretely (called springpot model). The constitutive equations of the springpot model and the creep compliance modulus were used to describe the property, particularly static property in creep $J(t)$. Eq. (1) represents the creep compliance modulus $J(t)$, obtained from the constitutive equation.

$$J(t) = \frac{1}{s * Gamma(1 + \alpha)} * t^\alpha \tag{1}$$

where, s is a related viscosity quasi-property, and α is the fractional order. s should be > 0 and α should be between 0 and 1 ($0 \leq \alpha \leq 1$) in order to be valid parameters in thermodynamics.

Generalized FMM is used for two springpot in series, which models more complex properties than springpot model. Starting from its constitutive equation of property, the generalized FMM have creep compliance, defined in Eq. (2) [19].

$$J(t) = \frac{1}{g} * \frac{t^\alpha}{Gamma(1 + \alpha)} + \frac{1}{m} * \frac{t^\beta}{Gamma(1 + \beta)} \tag{2}$$

These creep compliance equations present four parameters, two fractional orders α and β and two quasi-property parameters g and m, related to viscosity properties. Their thermodynamic validity depends on the following values, i.e., $\alpha(0 \leq \alpha \leq 1)$, $\beta < \alpha$, $g > 0$ and $m > 0$.

Three-parameter Gemant model is 1D SFVOF. Eq. (3) represents the creep compliance modulus [20].

$$J(t) = \frac{\tau}{v} \left(1 + \frac{\left(\frac{t}{\tau}\right)^\alpha}{Gamma(1 + \alpha)} \right) \tag{3}$$

where, v is the viscosity parameter, τ corresponds to relaxation time described by the model, and α is the power law-exponent [20]. v and τ should be > 0 and its fractional order should be between 0 and 1 in order to be valid parameters.

With the increasing use of recyclable materials, it is crucial to study how these components interact with a particular complicated model. Therefore, this paper aimed to comprehend how to apply a complex model to a physically heterogeneous material (rubber agglomerate material with urea TPE), study the number of parameters that works best in this situation and ultimately present the key equations, thus controlling the quality of these products. The methodology adopted by this paper was based on Ribeiro Alves's in 2020 excel adjustment technique, in which data was transformed into creep compliance tests and then modified using a pre-installed solver in pre-set beginning conditions. The generalized FMM was accepted in this instance, which had a specified margin of error. It was concluded that this paper achieved its goal and heterogeneous products were modeled successfully.

2 Methodology

In bachelor's thesis in chemistry, Alves [21] optimized the properties of rubber agglomerate using a DOE (Design of Experiments) essay. Six tests using an Instron Machine were conducted to test hardness (0.9 KN of indentation charge). Based on industrial production line, the Recauchutagem Nortenha SA laboratory showed a graphic of force vs. deformation of the six production samples, which were then evaluated at the University of Minho laboratory at 10 points per second and at 23°C room temperature. The specimens were 25mm wide in a square shape. Before weighing the pre-polymerized MDI and the rubber granules, the amount of water to be used in rubber agglomerate production was first calculated. The study prepared the rubber-MDI-water mixture, preheated the press to 110°C, applied the silicone Sarcosil commercial solution to a mold, and put the materials inside. When the temperature stabilized, the sample was put on press and removed after 8 to 15 minutes.

Alves provided the data for this study. Although all samples were tested, only the results of Sample 1 were addressed. Research results for each sample were very consistent and in the same magnitude range (Appendix A). Alves [21] altered the 1D SFVOF (with three parameters), the generalized FMM (with four parameters), and the Scott-Blair model (with two parameters), solved them using Excel's solver suite, and then determined statistically descriptive data, value sensibility and precision, and the outcome.

Excel program of Microsoft Office was used to modify Sample 1. Generalized Reduced Gradient (GRG) nonlinear was performed for nonlinear uniform problems of the solver, after the cell definition of objectives, the minimum value reducing the square difference between the experimental and adjusted model, variables, and thermodynamic constraints for each model. For the 100 population size, 0.000001 accuracy, automated rounding, and 0.00001 convergence were used. In addition, the variables were limited.

2.1 Adjustment Technique in Excel

Sample 1 contained Excel information on deformation unit and force unit for C104: D472. After using the information at 10 points per second, the time was translated to seconds. Then this paper built $J(t)$ using F104: F472

and placed the calculated model. In FMM, four blank cells were placed, which corresponded to the parameters. Then equation solution was written in the cell that represented the creep compliance of the FMM (Figure 5).

   This paper computed the difference between the experimental creep compliance modulus and the modified model, which was squared in another cell and added together in the final cell.

   The final solver command operated in the following manner: the squared sum of the differences between $J(t)$ was selected for the cell "definir objectivos" (defining objectives). The model that needed to be changed produced the smallest difference (minimo) between the corrected square difference. This paper first added variable cells and then four blank cells in the model. Thermodynamic constraints of the model ("sujeito as restriçoes") were selected using Generalised Reduced Gradient (GRG) nonlinear methods (see Figure 6).

Figure 5. Cell construction M116 in excel for adjusted FMM $J(t)$

Figure 6. Selection of parameters in the solver (Portuguese language)

3 Results

3.1 Parameters, Graphics and Equations Obtained from the Adjustments

3.1.1 Scott-Blair model/Springpot model

   Table 1 presents the parameter values obtained in Scott-Blair adjustment for Sample 1 of rubber agglomerate panel.

Table 1. Parameters obtained in Scott-Blair adjustment

Parameter	α	η
Value	0.099788118	156.26789004

Parameters in this model complied with the thermodynamic constraints, i.e., $\alpha (0 \leq \alpha \leq 1)$ and $\beta \geq 0$. Eq. (4) shows linear adjustment for the Scott-Blair model/Springpot model, which is not very in adaptation to the data (Figure 7).
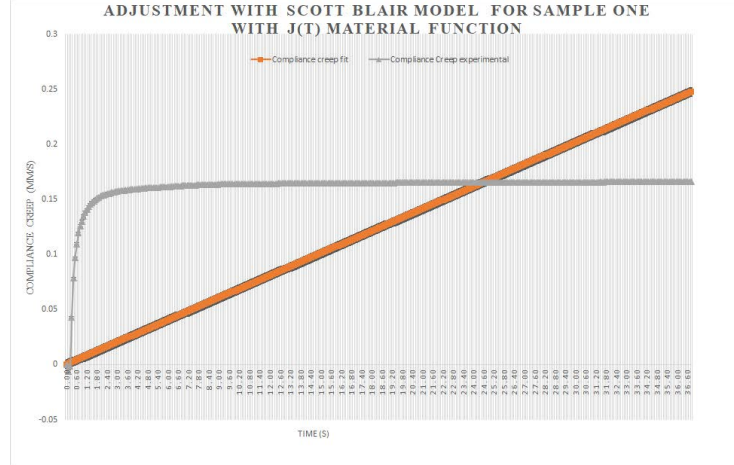
Figure 7. Adjustment of hardness test data of Ribeiro Alves using the Scott-Blair model

$$J(t) = \frac{1}{156 * Gamma(1.1)} * t^{1.1} \tag{4}$$

3.1.2 Figures and tables

Table 2 presents the values of the generalized FMM for Sample 1.

Table 2. Parameters obtained in the generalized FMM adjustment

Parameter	α	g	β	m
Value	0.10763	16.46144651	0.0202	13.97999397

It is observed that parameters obey the thermodynamic constraints imposed by the model, which means that $0 \leq \beta \leq \alpha \leq 1$ for the fractional orders and the viscosity quasi property tends to be > 0. Figure 8 shows a model, where experimental data is well modeled using the generalized FMM (Eq. (5)).

$$J(t) = \frac{1}{16.46} * \frac{t^{0.11}}{Gamma(1.11)} + \frac{1}{13.97} * \frac{t^{0.02}}{Gamma(1.02)} \tag{5}$$

3.1.3 1D SFVOF

Finally, Table 3 presents the parameters, obtained in 1D SFVOF for Sample 1. It is seen that α, β and τ comply with thermodynamic constraints.

Table 3. Parameters obtained in 1D SFVOF adjustment

Parameter	α	η	τ
Value	0.10251268	0.67264	0.036997898

Compared with the generalized FMM, comparable results were obtained after adjusting the 1D SFVOF. Although there were 3 parameters, the adjustment graphics were similar (Figure 9 and fitting Eq. (6)).
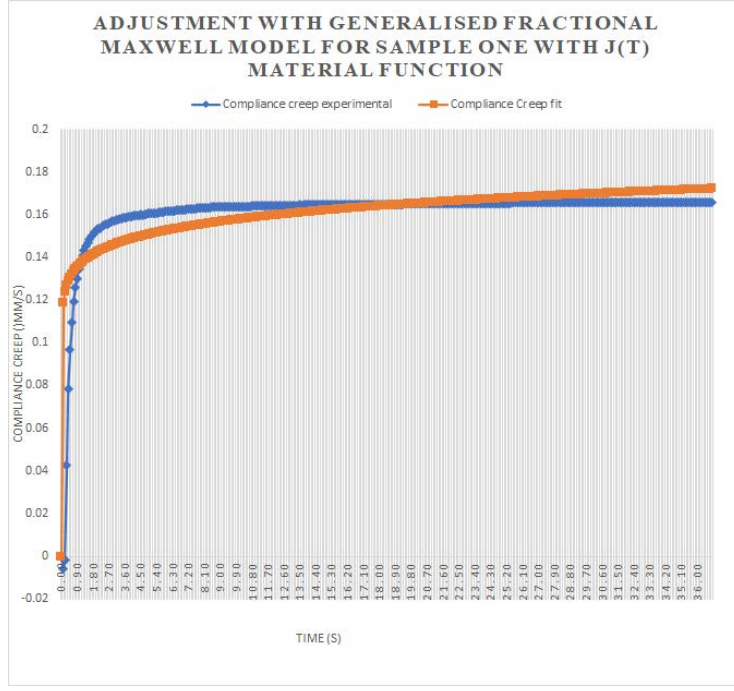
Figure 8. Adjustment of hardness test data of Ribeiro Alves using the generalized FMM
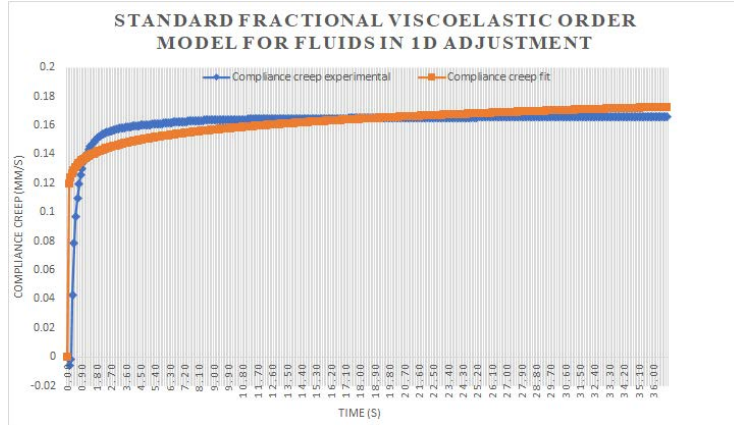
Figure 9. Adjustment of hardness test data of Ribeiro Alves using the standard viscoelastic order for fluids in 1D adjustment

$$J(t) = \frac{0.037}{0.67} \left(1 + \frac{\left(\frac{t}{0.037}\right)^{0.10}}{Gamma(1.10)} \right) \quad (6)$$

3.2 Hypotheses to Choose the Best Fitted Model

3.2.1 Univariate data analysis

Adjustment of the Scott-Blair model was not good, which caused the parameters not to be significant. The generalized FMM had very small quasi-property values and fractional orders. The 1D SFVOF required two small quasi-property values and a small fractional exponent.

However, this paper described the models, adjusted visually in Figure 8 (generalized FMM) and Figure 9 (1D SFVOF) using Analysis ToolPak add-in for Excel, which is a descriptive statistic analysis tool generating a univariate statisticcal report for data in the input range, and providing information on the central tendency and variability of data.

Table 4 presents the univariate data analysis for the $J(t)$ experimental and the $J(t)$ fit in the Scott-Blair model.

Table 5 represents the generalized FMM for both $J(t)$ experimental and $J(t)$ fit.

Table 4. Univariate statistics obtained in the Scott-Blair model adjustment

J(t) experimental (mm/s)		*J(t) fit* (mm/s)	
Mean	0.161569	Mean	0.124093
Standard error	0.000835	Standard error	0.00373
Median	0.164955	Median	0.124093
Mode	0.165	Mode	#N/A
Standard deviation	0.016015	Standard deviation	0.071548
Sample variance	0.000256	Sample variance	0.005119
Kurtosis	71.81194	Kurtosis	-1.2
Skewness	-7.95246	Skewness	$5.82E-16$
Range	0.171858	Range	0.246841
Minimum	-0.006	Minimum	0.000673
Maximum	0.165858	Maximum	0.247513
Sum	59.45757	Sum	45.66619
Count	368	Count	368
Confidence level (99.75%)	0.002542	Confidence level (99.75%)	0.011355

Table 5. Univariate statistics for the generalized FMM adjustment

J(t) experimental (mm/s)		*J(t) fit* (mm/s)	
Mean	0.161569	Mean	0.161597
Standard error	0.000835	Standard error	0.000503
Median	0.164955	Median	0.164385
Mode	0.165	Mode	#N/A
Standard deviation	0.016015	Standard deviation	0.009646
Sample variance	0.000256	Sample variance	$9.31E-05$
Kurtosis	71.81194	Kurtosis	2.148449
Skewness	-7.95246	Skewness	-1.42903
Range	0.171858	Range	0.053178
Minimum	-0.006	Minimum	0.119046
Maximum	0.165858	Maximum	0.172224
Sum	59.45757	Sum	59.46777
Count	368	Count	368
Confidence level (99.75%)	0.002542	Confidence level (99.75%)	0.001531

Table 6 shows $J(t)$ experimental and $J(t)$ fit for the 1D SFVOF adjustment.

Table 6. Univariate statistics for the 1D SFVOF adjustment

J(t) experimental (mm/s)		*J(t) fit* (mm/s)	
Mean	0.161569	Mean	0.161611
Standard error	0.000835	Standard error	0.000509
Median	0.164955	Median	0.164418
Mode	0.165	Mode	# N/A
Standard deviation	0.016015	Standard deviation	0.009772
Sample variance	0.000256	Sample variance	$9.55E-05$
Kurtosis	71.81194	Kurtosis	2.024806
Skewness	-7.95246	Skewness	-1.40224
Range	0.171858	Range	0.053351
Minimum	-0.006	Minimum	0.119093
Maximum	0.165858	Maximum	0.172443
Sum	59.45757	Sum	59.47279
Count	368	Count	368
Confidence level (99.75%)	0.002542	Confidence level (99.75%)	0.001551

The results of generalized FMM were better than that of the 1D SFVOF and even that of the Scott-Blair model.

3.2.2 Pearson correlation test

In Pearson correlation test, data between $J(t)$ adjusted and $J(t)$ experimental in the adjusted models was as exceptionally low as expected in the Scott-Blair model ($r^2 = 0.38004$), a little higher in the generalized FMM ($r^2 = 0.65688$) and the 1D SFVOF ($r^2 = 0.65258$). Therefore, the generalized FMM had the best results; the data adjusted using the Scott-Blair model was poorly correlated; another data was intermediately correlated.

Because the data was not linear, the values of r (Pearson coefficient) in this situation were not significant. However, the range of the r-value for each data was set from strongly positive to moderately positive (between 0.5-0.8). This analysis could not determine which model fit the data better once more.

3.2.3 Covariance analysis

In order to determine whether values were correlated, this paper made covariance analysis for the Scott-Blair model, the generalized FMM and the 1D SFVOF, as shown from Table 7 to Table 9.

Table 7. Covariance analysis for the Scott-Blair/Springpot model adjustment

	J(t) experimental	J(t) adjusted
$J(t)$ experimental	0.000325643	
$J(t)$ adjusted	0.000487289	0.005132978

Table 8. Covariance analysis for the generalized FMM adjustment

	J(t) experimental	J(t) adjusted
$J(t)$ experimental	0.000325643	
$J(t)$ adjusted	0.000171492	0.000163123

Table 9. Covariance analysis for the 1D SFVOF adjustment

	J(t) experimental	J(t) adjusted
$J(t)$ experimental	0.000325643	
$J(t)$ adjusted	0.000172144	0.000165562

Results of the generalized FMM had no bearing on the data of this paper, which meant that all the data corresponding to $J(t)$ experimental was not connected with $J(t)$ fit. First, this could be explained by the fluid models. Second, this could not be explained by data evaluation using a one-factor Analysis of Variance (ANOVA) before conducting additional tests.

3.2.4 One-factor ANOVA tests

Table 10 describes the one-factor ANOVA results for the Scott-Blair model.

Table 10. One-factor ANOVA results for the Scott-Blair model

Source of variation	S S	d f	M S	F	P-value	F crit
Between groups	0.258427	1	0.258427	96.14834	$2.06E-21$	3.854159
Within groups	1.97284	734	0.002688			
Total	2.231267	735				

Table 11 describes the one-factor ANOVA results for the generalized FMM.

Table 11. One-factor ANOVA results for the generalized FMM

Source of variation	S S	d f	M S	F	P-value	F crit
Between groups	$1.42E-07$	1	$1.42E-07$	0.00081	0.977304	3.854159
Within groups	0.128278	734	0.000175			
Total	0.128278	735				

Table 12 describes the one-factor ANOVA results for the SFVOF.

This paper examined the p-value and F value of this one-factor ANOVA based on its degrees of freedom. In this case, H0 represented a null hypothesis (i.e., all the means were equal), and H1 represented the alternative hypothesis

(i.e., means were not equal). With 735 degrees of freedom, the generalized FMM had a very low F-value and a very high p-value of probability ($p > 0.05$). The null hypothesis was not rejected because this paper considered the means of the population as equals. Thus, this test demonstrated that since there were no statistical differences between the means of each $J(t)$ experimental and $J(t)$ fit.

Table 12. One-factor ANOVA results for the SFVOF

Source of variation	S S	d f	M S	F	P-value	F crit
Between groups	$3.14E - 07$	1	$3.14E - 07$	0.001276	0.971517	3.854124
With groups	0.181254	736	0.000246			
Total	0.181255	737				

Similar situation was observed, i.e., the FMM had lower F value and higher p-value than the SFVOF. Therefore, this test supported the null hypothesis, because there were no discernible differences in any mean data of the 1D SFVOF.

At least some of these findings proved that the means were equal for each dataset and the mean data was not statistically significant. Additional tests should be conducted in order to determine whether these two models were more closely related than anticipated.

3.2.5 F-test analysis

F-test analysis aimed to understand the variance. Two sample distributions corresponding to the null hypothesis (H0) of this paper had equal variance, while that corresponding to the alternative hypothesis (H1) did not. The conclusions are shown in Table 13 (FMM) and Table 14 (1D SFVOF).

Table 13. F-test for the generalized FMM

	$J(t)$ experimental	$J(t)$ adjusted
Mean	0.161569	0.161597
Variance	0.000256	$9.31E - 05$
Observations	368	368
df	367	367
F	2.756352	
P(F≤f)one-tail	$9.65E - 22$	
F Critical one-tail	1.187611	

Table 14. F-test for the 1D SFVOF

	0	0
Mean	0.161569	0.161611
Variance	0.000256	$9.55E - 05$
Observations	368	368
df	367	367
F	2.685928	
P(F≤f) one-tail	$8.87E - 21$	
F Critical one-tail	1.187611	

Both covariance analysis and F-test revealed the variance problem of data and the sampled data, which meant that sample variance varied in such a way that P (F ≤ f) unilaterally approximated 0 for both the FMM and the 1D SFVOF. Therefore, this paper rejected the H0 and accepted the H1.

4 Discussion

This paper made three adjustments using three models, obtained their parameter values, adjustment graphics and equations. However, the adjusted functions were statistically investigated to confirm their homogeneity (F-test and one-factor ANOVA test), independence (Pearson correlation coefficient), and conformity (F-test and one-factor ANOVA test). The results showed that the means for both sample populations were equal, revealing data conformity and homogeneity. However, variance showed that the data range, which needed to be adjusted, was greater than that adjusted in each model, revealing less data conformity and homogeneity for the variance data.

These findings were consistent with the independence test, indicating that variance affected the Pearson correlation coefficient. The null hypothesis, where the variance was equal between experimental $J(t)$ and adjusted $J(t)$ for each model, was not rejected if the variance was closer to 1. The information might be remarkably independent.

In fact, this was possible because the rubber granulates shown in Figure 10 were a mix of a cellular material (mix of rubber from tires) and reacted urea TPE. Properties of the rubber agglomerate panel were crucial to the conclusions of this paper, because rubber enrobed with TPE slided between chains of rubber and urea TPE. The rubber agglomerate with urea TPE also contained air, which may tamper with data values when released. Due to the above-mentioned defaults in rubber production, such as rubber or urea chains caused by heat degradation, a complex equation with few parameters possibly did not perform as well as observed. The FMM with a certain margin of error was accepted because the 1D SFVOF had comparable homogeneity and conformity but higher independence.

Figure 10. Example of a finished rubber agglomerate sample

5 Conclusions

For rubber agglomerate panel, the generalized FMM fit the data the best, compared with the Scott-Blair model and the 1D SFVOF. The generalized FMM, with a certain margin of error, could be used for constructing the rubber agglomerate panel using Salvadori equipment.

It's critical to realize how flawless nature is. Although certain properties are more complex than others, this paper believes that all aspects of properties in the universe can be represented by various mathematical equations. This paper only found the homogenous material of melted polymer during investigation and literature review. Another heterogeneous material like this was never noticed in the years of investigation. Therefore, this accomplishment explained why it did not function. However, if parameters can be carefully monitored in future manufacturing of rubber agglomerate, it will be feasible to identify a suitable model.

It is likely that the outcome for this material is not too awful because there are other aspects involved in rubber production, such as formulation, machine parameters, and personnel performance. However, according to Professor Mainardi Francesco, the future lied on the new models, and more models should be examined, based on modified models and Bessel functions.

Data Availability

The data used to support the findings of this study are available from the corresponding author upon request.

Conflicts of Interest

The author declares that he has no conflicts of interest.

References

[1] D. P. Harper, "The evaluation of 4-4' diphenylmethane diisocyante cure in a saturated steam environment," Master's thesis, Washington State University, U.S, 1998.

[2] "Equipment to transform recycled rubber into finished products," https://www.salvadori.com/recycling/our-equipment/, 2023.

[3] "Rheos-rheology, open-source," https://juliarheology.github.io/RHEOS.jl/stable/#RHEOS-RHEology,-Open-Source, 2023.

[4] J. L. Kaplan, A. Bonfanti, and A. J. Kabla, "RHEOS.jl-A julia package for rheology data analysis," *J. Open Source Softw.*, vol. 4, no. 41, p. 1700, 2019. https://doi.org/10.21105/joss.01700

[5] A. Bonfanti, J. L. Kaplan, G. Charras, and A. Kabla, "Fractional viscoelastic modelsfor power-law materials," *Soft Matter*, vol. 16, no. 26, pp. 6002–6020, 2020. https://doi.org/10.1039/DOSM00354A

[6] B. M. R. Alves, "Modelizacao viscoelastica fracionaria do comportamento em relaxacao da resina polimerica de ABS com software R," *RCT-Rev. Ciencia e Tecnol.*, vol. 6, 2020. https://doi.org/10.18227/rct.v6i0.5844

[7] B. M. R. Alves, "Estudo e afericao da qualidade de ajustes de modelos viscoelasticos em ensaios dinamicos para o polibutadieno com o software commercial office," *RCT-Rev. Ciência e Tecnol.*, vol. 8, 2022.

[8] B. M. R. Alves, "Modeling insite® technology ethylene α-olefin resins with standard fov fluid in 1D," *J. King Saud Univ.-Eng. Sci.*, vol. 31, no. 2, pp. 157–163, 2019. https://doi.org/10.1016/j.jksues.2017.01.001

[9] "Gnu-octave," https://octave.org/, 2023.

[10] "Matlab-mathworks," https://ch.mathworks.com/products/matlab.html, 2023.

[11] "Data analysis, statistical and process improvement tools," https://www.minitab.com/en-us/, 2023.

[12] "Spss statistics," https://www.ibm.com/products/spss-statistics, 2023.

[13] P. J. Doerpinghaus Jr, "Flow behavior of sparsely branched metallocene-catalyzed polyethylenes," Ph.D. dissertation, Virginia Polytechnic Institut and State University, Blacksburg, VA, USA, 2002.

[14] C. W. Macosko, *Rheology: Principles, measurements and applications*. Wiley, 1996.

[15] R. C. de Oliveira, R. M. Rossi, and S. T. D. de Barros, "Estudo reológico da polpa de morango (fragaria vesca) em diferentes temperaturas," *Acta Sci. Technol.*, vol. 34, no. 3, pp. 283–288, 2012. https://doi.org/10.4025/actascitechnol.v34i3.7833

[16] T. R. D. S. Mathias, K. C. S. Andrade, C. L. D. S. Rosa, and B. A. Silva, "Avaliação do comportamentoreológico de diferentes iogurtes comerciais," *Braz. J. Food Technol.*, vol. 16, pp. 12–20, 2013. https://doi.org/10.1590/S1981-67232013005000004

[17] T. C. B. McLeish and R. G. Larson, "Molecular constitutive equations for a class of branched polymers: The pom-pom polymer," *J. Rheol.*, vol. 42, no. 1, pp. 81–110, 1998. https://doi.org/10.1122/1.550933

[18] F. Mainardi, *Fractional calculus and waves in linear viscoelasticity*. World Scientific, 2022.

[19] A. Jaishankar and G. H. McKinley, "Power-law rheology in the bulk and at the interface: quasi-properties and fractional constitutive equations," *Proc. R. Soc. A*, vol. 469, no. 2149, 2013. https://doi.org/10.1098/rspa.2012.0284

[20] NASA, "Fractional order viscoelasticity (FOV): Constitutive development using the fractional calculus: First annual report," USA, Tech. Rep. NASA/TM-2002-211914, 2002.

[21] B. M. R. Alves, "Hardness experiment results for rubber agglomerates," Mendeley Data, https://doi.org/10.17632/hzzjxpdfmg.2, 2019.

Nomenclature

$J(t)$	creep compliance modulus, $\mathrm{mm/s}$
TPE	thermoplastic Elastomer
$N1$	first-order normal stress differences
$N2$	second order normal stress difference

Greek symbols

ε	deformation, mm
β	Power-Law exponent (dimensionless)
α	Power-Law exponent (dimensionless)